Probing the Interaction of Poly(vinylpyrrolidone) with Platinum Nanocrystals by UV−Raman and FTIR

Yuri Borodko,[†] Susan E. Habas,[‡] Matthias Koebel,[†] Peidong Yang,[†,‡] Heinz Frei,[§] and Gabor A. Somorjai*[,†,‡]

Materials Sciences Division, Lawrence Berkeley National Laboratory, Berkeley, California 94720, Department of Chemistry, University of California, Berkeley, California 94720, and Physical Biosciences Division, Lawrence Berkeley National Laboratory, Berkeley, California 94720

Received: May 30, 2006; In Final Form: September 11, 2006

The vibrational spectra of platinum nanoparticles (2.4−9 nm) capped with poly(*N*-vinylpyrrolidone) (PVP) were investigated by deep UV−Raman and FTIR spectroscopy and compared with those of pure PVP. Raman spectra of PVP/Pt show selective enhancement of C═O, C−N, and CH_2 vibrational modes attributed to the pyrrolidone ring. Selective enhancement of ring vibrations is attributed both to the resonance Raman effect and SERS chemical enhancement. A red shift of the PVP carbonyl frequency on the order of 60 cm^{-1} indicates the formation of strong >C═O−Pt bonds. It is concluded that PVP adheres to the nanoparticles through a charge-transfer interaction between the pyrrolidone rings and surface Pt atoms. Heating the Pt nanoparticles under reducing conditions initiates the decomposition of the capping agent, PVP, at a temperature 100 °C below that of pure PVP. Under oxidizing conditions, both PVP/Pt and PVP degrade to form amorphous carbon.

Introduction

"Platinum blue" and "platinum tan" coordination compounds with 2−8 platinum atoms arranged as a bridging chain have attracted much interest over the past decade. Many binuclear and tetranuclear Pt compounds stabilized by amide bridging ligands have been isolated and structurally characterized.[1] Crystallographic studies of Pt−pyridone and Pt−pyrrolidone complexes show that amide groups usually bind (through O or N) to mixed valence Pt−Pt bridge sites with average Pt oxidation states of Pt^{2+}, $Pt^{2.25+}$, $Pt^{2.5+}$, and Pt^{3+}. An increase of the formal Pt oxidation state from Pt^{2+} to Pt^{3+} is reflected in the increase of Pt−Pt bridge distance from 2.6 to 2.95 Å[2]. These coordination compounds possess attractive chemical properties that include unusual structural flexibility of the Pt chain depending on oxidation state,[2,3] interesting catalytic behavior such as the ability to act as one step, two-electron reductants,[4] or activity as antitumor agents.[5,6]

In light of these properties, it may not be surprising that the polymeric form of vinylpyrrolidone, PVP, has been used extensively as a macroligand for stabilizing Pt, particularly in the form of nanocrystals.[7,8] More specifically, PVP has been used as a shape-controlling reagent in the PVP-mediated polyol process to produce metallic nanostructures with different shape,[8a] and as a flexible membrane around metallic colloids, which influences the selectivity of catalytic reactions.[8b] The integration of PVP/Pt nanoparticles in catalytic reactions has introduced new opportunities to create tailored catalytic systems. In addition to the control that PVP can provide over nanoparticle size and shape, the size and structure of polymeric shell, e.g., altering the molecular weight of PVP and degree of PVP cross-linking, can also be systematically changed, as shown in Figure 1. However, very little is known about the structure and nature of the chemical bond between PVP and platinum nanocrystals at the molecular level. Different experimental techniques have been used to explore the interface of PVP/Pt including XPS,[9] UV−vis,[9a] FTIR,[9] and Raman spectroscopy.[9b]

In this paper we report a study of PVP-capped Pt nanocrystals using deep UV−Raman and FTIR spectroscopy. Deep UV−Raman spectroscopy can be advantageous for probing the interaction between PVP and the Pt surface because of the substantial intensity enhancement expected for some vibrational modes as a result of both the resonance Raman and chemical enhancement effects of SERS. We were able to differentiate between modes arising from unbound PVP and polymer interacting with surface Pt atoms of nanoparticles. Some vibrational modes of the pyrrolidone rings in deep UV−Raman (244 nm) are enhanced due to resonance Raman and chemical enhancement of SERS, making the amide groups in PVP sensitive probes for the interaction of PVP with the Pt nanocrystals. We have also studied the thermal and chemical degradation of pure PVP and PVP coated Pt nanocrystals in hydrogen and oxygen.

Experimental Section

Synthesis of Shape-Controlled Platinum Nanocrystals by Ethylene Glycol Reduction. Platinum cubes (9.4 ± 0.6 nm, 80%) were synthesized by adding 0.5 mL of 2×10^{-3} M silver nitrate ($AgNO_3$) solution in ethylene glycol (EG) to refluxing EG followed by stepwise addition of poly(*N*-vinylpyrrolidone) and hexachloroplatinic acid ($H_2PtCl_6 \cdot 6H_2O$) solutions in EG. The resulting mixture was heated under reflux for an additional 5 min followed by centrifugation. A more detailed description of the experimental procedure can be found elsewhere.[8] After separation of the supernatant and precipitate in acetone, the latter

[†] Materials Sciences Division, Lawrence Berkeley National Laboratory.
[‡] University of Californiay.
[§] Physical Biosciences Division, Lawrence Berkeley National Laboratory.

10.1021/jp063338+ CCC: $33.50
Published on Web 10/25/2006

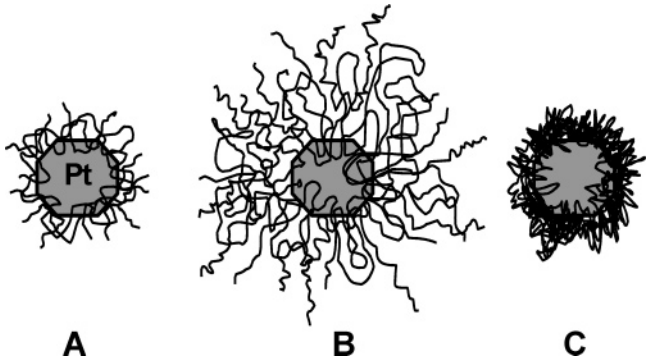

Figure 1. Schematic illustration of PVP/Pt nanoparticles with different structure (morphology) of capping polymeric macroligand: (A) low molecular weight PVP, (B) high molecular weight PVP, and (C) dense, cross-linked PVP.

was redispersed and washed twice with ethanol and finally dispersed in ethanol or chloroform. Nanoparticles obtained in the absence of silver ions were predominantly cubic (8.7 ± 1.2 nm, 80%) (Figure 2).

Synthesis of PVP-Capped Platinum Nanoparticles by Ascorbic Acid Reduction. PVP stabilized platinum nanoparticles with a mean diameter of 5.3 nm were synthesized by the direct reduction of $H_2PtCl_6 \cdot 6H_2O$ with ascorbic acid in a water/methanol solvent mixture. The platinum precursor was added to a refluxing solution of PVP and ascorbic acid under vigorous stirring. A color change from yellow to dark brown within a few minutes indicated the formation of nanoparticles. After a 15-min reaction time, the solution was cooled to room temperature and isolated by precipitation with acetone. Excess PVP was removed by repeated suspension (4−6 times) of the particles in ethanol and precipitation with hexanes. The final product was then dispersed in ethanol.

A dilute solution of the purified sample was applied onto a 200 Mesh Formvar/C coated Cu-grid and dried in air. TEM analysis was carried out with a Tecnai 12 Transmission Electron Microscope operated at 100 kV acceleration voltage.

Spectroscopic Characterization. All UV−vis absorption spectra were measured in water on an Agilent 8453 UV−visible ChemStation equipped with a 1 cm path length quartz cuvette. FTIR-DRIFT spectra were measured with a Nicolet Nexus-670 spectrophotometer with integrated diffuse reflectance optics (Spectra-Tech Collector II). We found that improved spectra could be obtained by using a thin layer of PVP/Pt evaporated from chloroform or ethanol solution on a reflective surface such as aluminum or gold foil in place of the standard DRIFT sample holder. Since the layer thickness can be adjusted so as to render the sample partially IR transparent, we were able to optimize the ratio of diffuse to specular reflectance and obtain spectra of similar quality compared to those measured in transmission mode. This method can be described as a hybrid of DRIFT and IR reflection absorption spectroscopy (IRRAS). The temperature/vacuum chamber Spectra-Tech 0030-101 was used for in situ FTIR measurements in H_2/Ar (10% H_2) flow.

The deep UV−Raman spectroscopy system is shown in Figure 3. A continuous wave (cw) intracavity doubled argon ion laser operating at 244 nm is used as the excitation source. A custom designed (Omega Optical) UV long-pass edge filter is used to block plasma lines below 246 nm. A 37 mm focal length fused silica lens allowed focusing of the laser on a ~500 μm spot on the surface of the sample. Backscattered light was collected with the same lens, collimated, and directed to the entrance slit of a triple spectrometer Spex 1877C, which was optimized for performance in the deep UV region. Some spectra were taken with an additional band-pass filter in front of the spectrometer to further reduce the intensity of elastically scattered radiation. Spectra were recorded with an LN_2-cooled, UV-enhanced CCD camera. The instruments dispersion is 2.1 cm^{-1}/pixel; the typical resolution of 12 cm^{-1} was controlled by the slit width of the dispersion stage of the triple spectrometer.

Deep-UV irradiation of PVP is known to induce intra- and intermolecular cross-linking of the polymer chains.[10] To eliminate modification or decomposition of PVP/Pt samples under UV irradiation we used a custom designed rotating sample holder (1200 rpm) equipped with a second motor for lateral translation (240 rpm). In this manner, the laser was XY-rastered over the entire sample, decreasing the UV exposure in a given spot by 10^3 when compared with a static sample holder. No detectable photodegradation of samples was observed in this configuration over a period of 90 min.

To prepare samples for the Raman study, solutions of PVP/Pt in chloroform were evaporated on 30 mm diameter Al foil substrates. Typical collection times were 5−30 min, using 3−5 mW of 244 nm excitation energy. An oil-free Alcatel Drytel 34 turbo-pump station was used for sample evacuation. GRAMS/AI software from Thermo Galactic was used for processing UV−Raman and FTIR-DRIFT spectra.

Results and Discussion

Vibrational Spectra of Neat PVP. The vibrational spectrum of pure PVP has been studied previously with IR and Raman techniques. It was shown that increasing the molecular weight from 3 000 to 2 000 000, i.e., the number of repeating units, did not induce any substantial changes in the Raman spectra.[11]

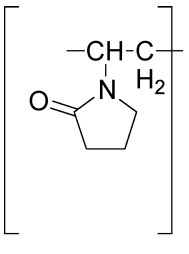

Also, the FTIR spectra of soluble and cross-linked PVP are very similar.[12] Figure 4 shows the FTIR and UV−Raman spectra of pure PVP55 (MW 55 000) in the region of 500−3700 cm^{-1}. The presence of a heteroatom and a carbonyl group in the pyrrolidone ring sufficiently decreases the symmetry so that the majority of vibrational modes are present in both the IR and Raman spectra, although with different intensities (Figure 4A). It has been shown that the frequency of the carbonyl stretch is very sensitive to hydrogen bond formation with water molecules. As the concentration of adsorbed water is increased, the ν(C=O) shifts from 1680 to 1652 cm^{-1}.[11,13] A comparison of the IR and Raman C−H stretching modes shown in Figure 4B makes it possible to identify five peaks corresponding to the ν_s and ν_{as} (CH_2) stretch of the pyrrolidone ring as well as $\nu(CH_2)$ and the tertiary C−H stretch of the backbone. Deconvolution of the Raman spectrum for PVP in this spectral region is depicted in Figure 5A. The weak Raman line at 3300 cm^{-1} corresponds to the first overtone of the carbonyl stretch (Figure 5B). Empirical assignments of IR and Raman lines of pure PVP are summarized in the first two columns of Table 1.

Excitation with 244 nm radiation did not induce selective enhancement of any vibrational mode intensities indicating that for pure PVP we detect a "normal" Raman spectrum. The deep

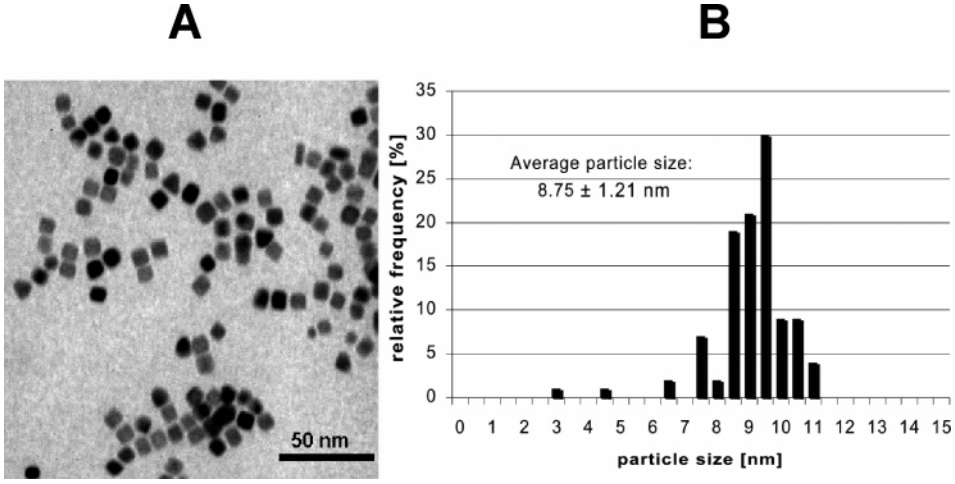

Figure 2. TEM analysis of ethylene glycol reduced PVP stabilized Pt nanoparticles: (A) TEM image of predominantly cubic platinum nanoparticles (8.7 ± 1.2 nm, 80%) synthesized in the absence of silver ions and (B) corresponding size histogram.

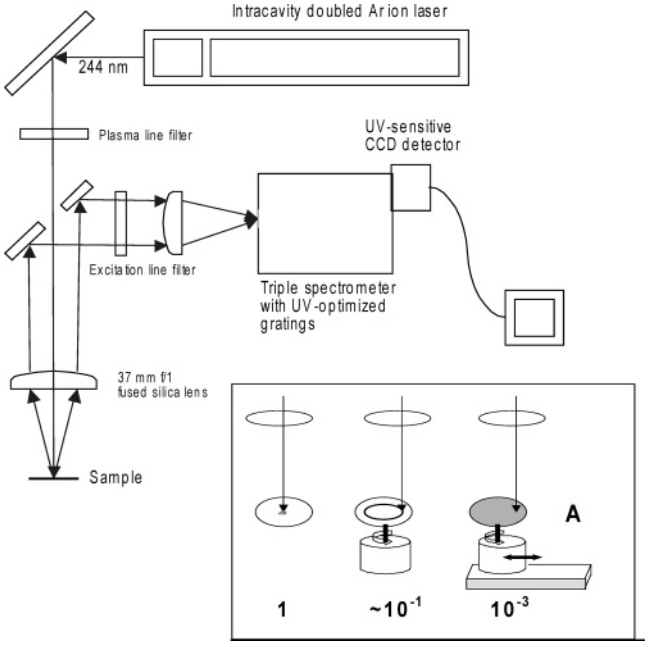

Figure 3. Overview of UV−Raman spectroscopy system: (A) special XY-moving sample holder allows decrease UV-irradiation dose by a factor of about 10^3 compared with standard static holder.

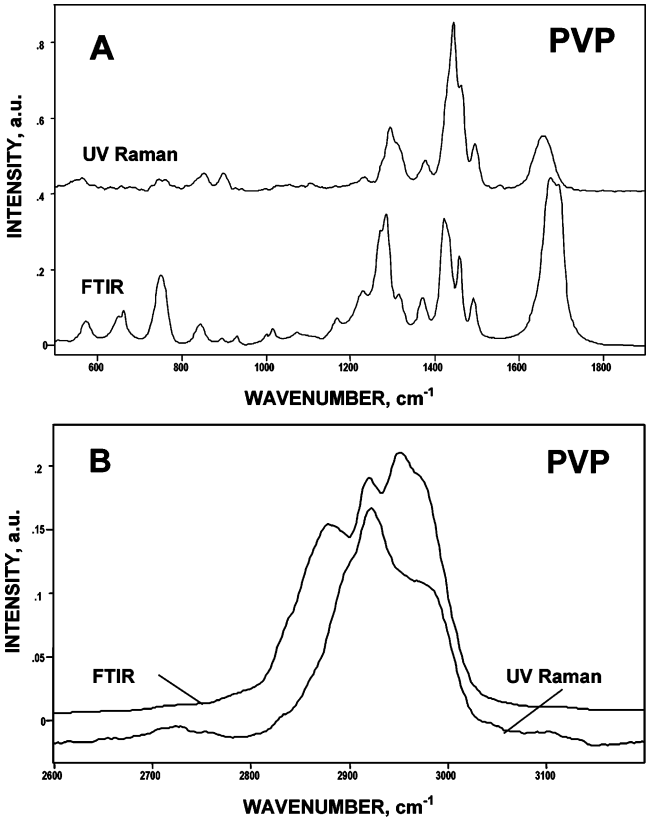

Figure 4. UV Raman and FTIR spectra of pure PVP: (A) overview of UV−Raman and FTIR spectra of PVP in the region of 550−3200 cm^{-1} and (B) comparison of Raman and FTIR spectra of PVP in the region of C−H stretch.

UV−Raman (244 nm) spectrum of PVP is similar to previously measured PVP spectra obtained with laser excitation at 488 nm,[13] 632.8 nm,[14] and 1064 nm.[11] As further evidence that no enhancement occurs, the ratio of intensities I(C═O)(1660) to I(CH_2 bend)(1442) are consistently less than 1 for all excitation lines in the range of 244−1064 nm.

UV Raman and FTIR Spectra of PVP/Pt. The UV−Raman spectra of pure PVP and PVP-capped Pt nanocrystals (2.4 nm, random shape) differ noticeably (Figure 6A). A dominant intense line appears at 1606 cm^{-1} with a weak shoulder at 1660 cm^{-1}. The ratio of intensities of I(C═O) to I(CH_2 bend) becomes I(1606) > I(1442), which is opposite to the ratio for pure PVP. Additionally, the CH_2 bending region is dramatically perturbed with the strongest line now at 1380 cm^{-1}. The C−H and O−H stretch region of PVP/Pt (25 °C in air), shown in trace 1 of Figure 6B, has peaks at 2930, 3206, and 3450 cm^{-1}. Heating the sample at 70 °C in air for 30 min resulted in a decrease in the intensity of the broad line at 3450 cm^{-1} relative to that at 2930 cm^{-1} (Figure 6B, trace 2). This broad line is attributed to the OH stretch of hydrogen-bonded water,[11] while the peak at 3206 cm^{-1} is assigned to the first overtone of the carbonyl group vibration at 1610 cm^{-1}. Furthermore, comparison between the Raman spectra of pure PVP and PVP/Pt shows that the ratio of intensity of the overtone at 3206 cm^{-1} to the fundamental CH_2 stretch at 2930 cm^{-1} is substantially larger for PVP/Pt. The appearance of intense lines in the UV−Raman spectrum of PVP/Pt is most probably a result of resonance Raman enhancement of specific vibrational modes of PVP moieties that interact with platinum. Although steric considerations suggest that the number of pyrrolidone rings interacting with the Pt surface must be small in comparison with noninteracting rings, the selective enhancement of vibrational modes associated with chromophoric groups

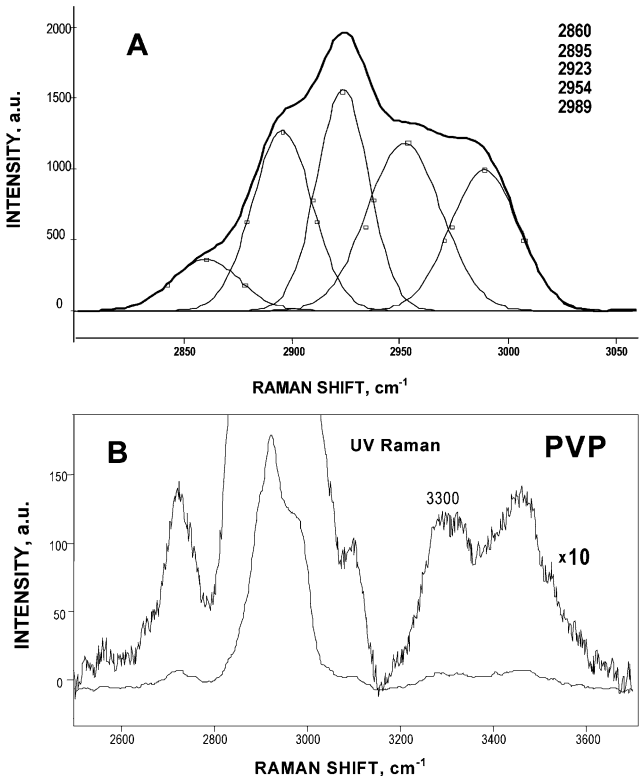

Figure 5. (A) Deconvolution of experimental Raman C−H stretch line of PVP using GRAMS/AI software from Thermo Galactic. (B) UV Raman spectra of PVP in the region of 2500−3700 cm^{-1}, and the same spectrum expanded 10-fold.

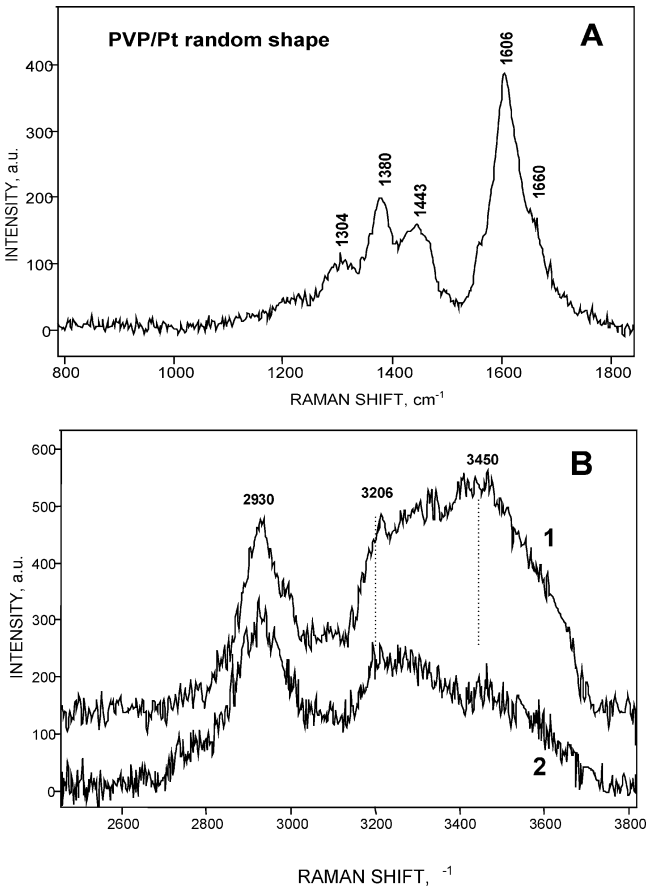

Figure 6. UV−Raman spectra of PVP/Pt (random shape, 2.6 nm): (A) spectrum of PVP/Pt in the region of amide stretch and CH_2 bending vibrations and (B) spectra of PVP/Pt at 25 °C (1) and PVP/Pt heated at 70 °C for 20 min in air (2) in the region of 2500−3800 cm^{-1}. After heating, the line intensity of adsorbed water at 3450 cm^{-1} decreased while the intensity of the first overtone at 3206 cm^{-1} did not change.

that are adsorbed on the metal surface is sufficiently large to result in an intense spectrum of these Pt-coordinated groups.

The UV−Raman spectrum shown in Figure 7 for cubic Pt nanocrystals (7 nm) capped with PVP has two intense bands at 1605 and 1640 cm^{-1} attributed to the carbonyl stretch (Figure 7A), and an intense doublet at 3206, 3270 cm^{-1} corresponding to the first overtone of the ν(C═O) stretch with a line shape reminiscent of the fundamental ν(C═O) mode (Figure 7B). The intensity of the first overtone of the ν(C═O) at 3300 cm^{-1} for pure PVP is about 5% of the intensity of the nearby fundamental CH_2 stretch (Figure 5B). By contrast, the spectrum for PVP/Pt (7 nm, cubes) exhibits intensities of the fundamental CH_2 stretch and the first overtone of the ν(C═O) that are equal in magnitude (Figure 7B), indicating that the overtone transition is dramatically enhanced by coordination to Pt. It is worth noting that the shape of the C−H stretch absorptions for pure PVP and PVP/Pt (cubic) is different, as shown on an expanded scale in Figure 8A. Detailed comparison of the profile of FTIR and Raman bands makes it possible to distinguish five components for pure PVP, which are attributed to the CH_2 stretch modes $\nu_s(CH_2)$ and $\nu_{as}(CH_2)$ of the pyrrolidone ring, $\nu_s(CH_2)$ and ν_{as}-(CH_2) for the polymer backbone, and the tertiary C−H stretch (Figure 5A and Table 1). The Raman spectrum for PVP/Pt (cubic), however, has only three C−H stretch peaks at 2860, 2902, and 2963 cm^{-1} according to the deconvolution shown in Figure 8B. The prominence of these three peaks suggests that there is an interaction between the platinum surface and the amide group of the pyrrolidone rings and this charge-transfer coupling influences the CH_2 vibrations of the rings. The three CH stretching modes in the UV−Raman of PVP/Pt may be assigned to $\nu_{as}(CH_2)$ and $\nu_s(CH_2)$ of the pyrrolidone ring, and tertiary C−H of the backbone (Table 1).

The structure of PVP adsorbed on platinum nanoparticles varies during heating in air. Recently it was shown that above 150 °C PVP undergoes thermal densification as a result of cross-linking.[15] A sample of PVP/Pt that was heated at 200 °C for 20 min in air shows a ν(C═O) overtone intensity that increased to the size of the fundamental line (Figure 9). The increase in

TABLE 1: Poly(vinylpyrrolidone) IR and UV-Raman Line Assignments

IR PVP	Raman PVP	Raman PVP/Pt	assignment[12,26,29]
3342	3300	3305 3206	2 × (C═O)
2976	2989		asym CH_2 stretch, chain
2950	2954	2963	asym CH_2 stretch, ring
2922	2923		sym CH_2 stretch, chain
	2895	2902	sym CH_2 stretch, ring
2873	2860	2860	C−H stretch
1695 1674	1662	1640 1606	amide C═O, C−N stretch
1492 1461 1430	1494 1462 1445	1500 1442	C−N CH_2 sissor
1371	1380	1380	CH bend
1315 1280	1296	1300	CH_2 wag, C−N stretch
1229 1167			CH_2 twist
1017 930 844 750	1023 900 851 754		C−C, CH_2 rock C−C, ring breathing C−C ring C−C chain
654 573	560		N−C═O bend, ring def.

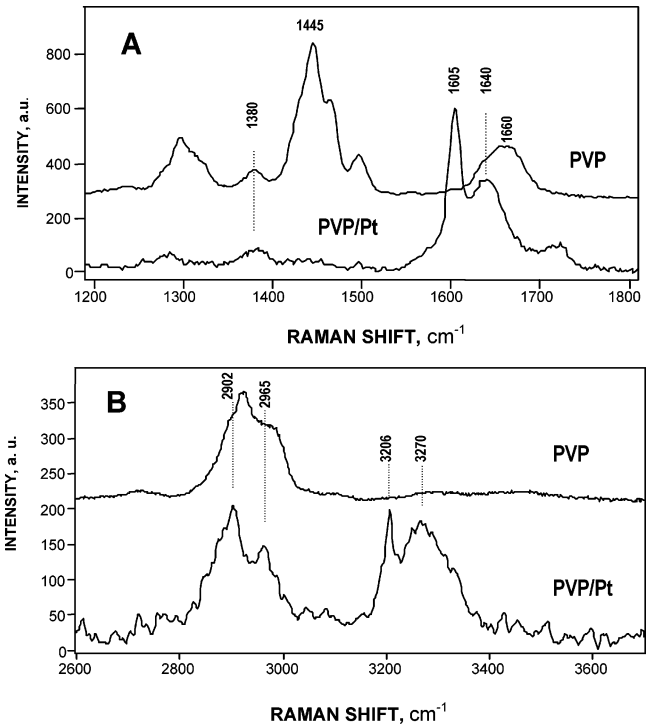

Figure 7. UV−Raman spectra of PVP/Pt (cubes nanocrystals, 7 nm) and pure PVP: (A) spectrum of PVP/Pt and spectrum of powdered PVP in the region of 1200−1800 cm^{-1} and (B) spectra of PVP/Pt cubes and PVP in the region of 2600−3700 cm^{-1}. Attention is drawn to the fact that the intensity of the amide first overtones at 3200−3270 cm^{-1} is as strong as that for the fundamental CH_2 stretching vibrations.

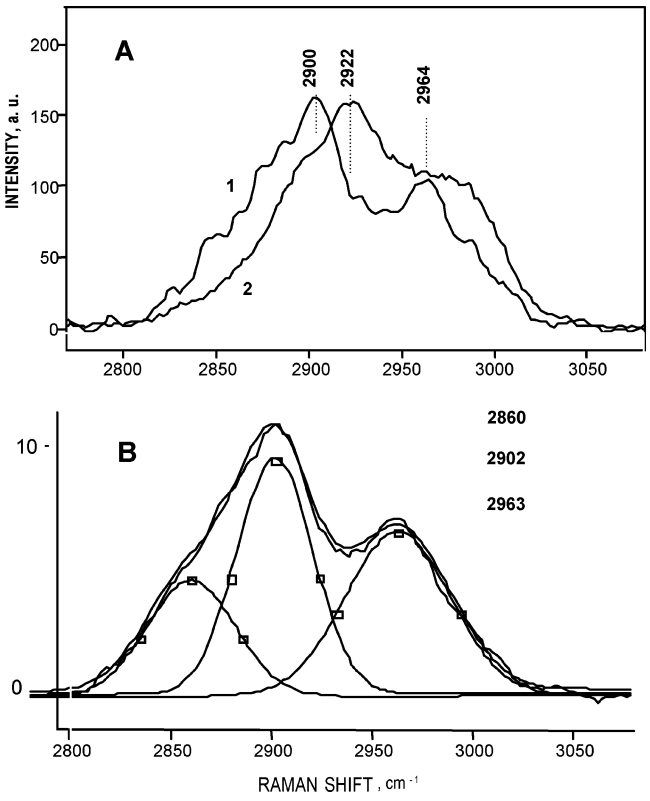

Figure 8. Comparison of the shapes of C−H stretch absorptions: (A) Raman lines of PVP/Pt (cubes, 7 nm) (1) and powdered PVP (2) in the region of 2750−3100 cm^{-1} and (B) deconvolution of the C−H stretch Raman line of PVP/Pt (cubes, 7 nm).

intensity of the first ν(C═O) overtone suggests that the structure of the capping PVP becomes denser at higher temperatures,

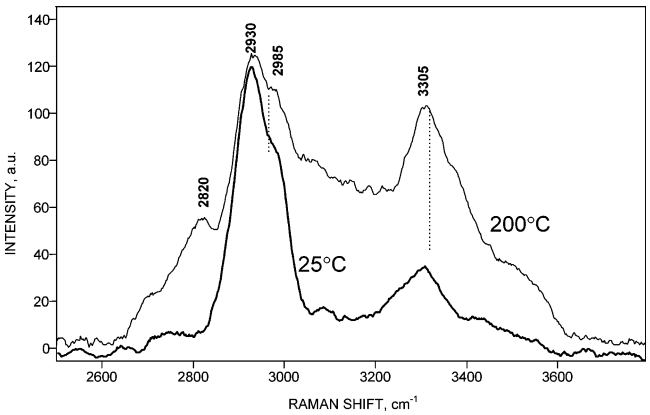

Figure 9. Effect of heating on UV−Raman spectra of PVP capping Pt nanocrystals with cubic shape, 7 nm. Synthesis of Pt nanocrystals was performed with ascorbic acid as reductant. Comparison of the spectra of PVP/Pt at 25 °C and after heating at 200 °C in air for 20 min in the region of 2500−3800 cm^{-1} indicates that the intensity of the first overtone of the carbonyl stretch at 3305 cm^{-1} increased under heating. Heating increases the cross-linking of capping PVP, resulting in the rise of the number of Pt ← amide group contacts and a concurrent increase of the intensity of the carbonyl first overtone due to the SERS effect.

thereby increasing the number of contacts between the pyrrolidone rings and the platinum surface (Figure 1C).

Chemical Nature of Surface Enhanced Raman Scattering. The UV−vis absorption spectra of pure PVP and PVP/Pt differ notably at 244 nm, which corresponds to the laser excitation wavelength for the UV−Raman studies. Platinum nanocrystals capped with PVP absorb strongly at 244 nm while pure PVP does not exhibit perceptible absorption (Figure 10). Recently it was shown that the UV−vis spectrum of the PVP/Pt exhibits absorption at 215 nm as a result of an interband (d-sp) transition with a small contribution from plasmon oscillations, and a second absorption band near 260 nm assigned to clusters of nanoparticles.[9a] The resonance Raman enhancement of vibrational modes of the amide group and ring vibrations observed here indicates that the 244 nm excitation line lies within the absorption band that originates from charge transfer (CT) between Pt and the pyrrolidone rings of PVP, although its strength may be too low for detection.[16]

The selective detection of vibrational modes associated with pyrrolidone rings interacting with platinum nanoparticles by UV−Raman (244 nm) occurs as a result of two enhancement effects: the resonance Raman effect and CT or chemically enhanced SERS (Figure 10A).[17] The chemically enhanced Raman scattering refers to a "first-layer" chemical enhancement.[18] Electronic coupling between adsorbed molecules and surface atoms of a metal is known to increase the scattering cross section of Raman lines associated with CT chromophoric groups.[17] This model may be applied for analysis of UV−Raman (244 nm) spectra for the PVP/Pt system based on the following observations: (i) the pyrrolidone rings of PVP interact strongly with Pt surfaces via the carbonyl group as indicated by the 50 cm^{-1} red shift of ν(C═O); (ii) the appearance of a new UV absorption at 244 nm and selective enhancement of pyrrolidone ring vibrational modes; and (iii) the intensity of the first overtone of ν(C═O) is very strong and becomes comparable in intensity to the fundamental mode. The last point is in agreement with theoretical consideration of the CT-SERS effect. For a strong charge-transfer interaction between an adsorbed chromophore and a metal, the Franck−Condon transition associated with the displaced potential energy minimum (ΔQ) along the normal coordinate is expected to result in an increase of the intensity of the first overtones[19,20] as depicted in Figure 10B. We conclude that the observed intensity of the first overtone of ν(C═O) at

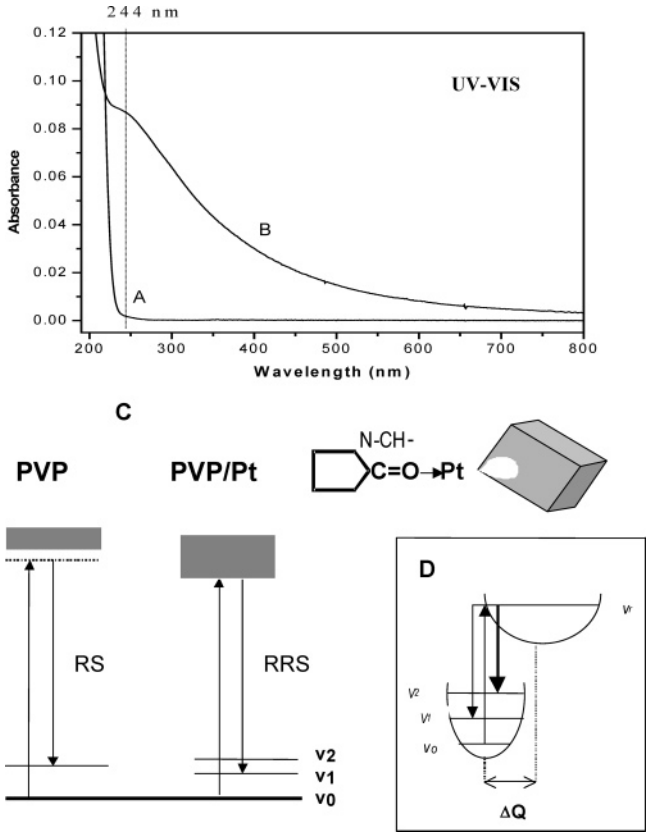

Figure 10. (A and B) UV−vis spectra of PVP and PVP/Pt cubes in water. The dotted vertical line shows that excitation laser line 244 nm is within the strong absorption band of PVP/Pt with $\lambda \approx 250$ nm. (C) Schematic diagrams of transitions for "normal" Raman effect (RS) in the case of PVP, and for SERS (chemical charge-transfer enhancement) that is characteristic of PVP/Pt. (D) Potential energy diagram for the ground and resonant excited states showing the case when at definite shift parameter ΔQ the intensity of the first overtone becomes comparable or more to that of the fundamental.[18,19]

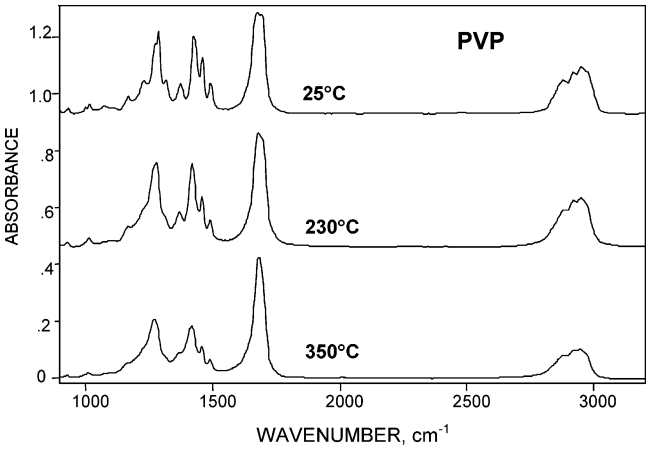

Figure 11. Overview of FTIR in situ spectra of PVP at raising temperature with heating rate 2 deg/min in H_2/Ar (10% H_2) flow in the temperature range of 25−350 °C.

3300 cm^{-1} in the PVP/Pt system is in agreement with the theoretical prediction that overtone intensity for adsorbed molecules on a metal surface with strong CT interaction may be as strong as the fundamental mode.[20,21]

FTIR measurements of PVP/Pt further corroborate the conclusion that selective UV enhanced Raman vibrational modes may be assigned to "first-layer" chemically bonded pyrrolidone rings. Unlike the UV−Raman spectrum, the FTIR spectrum of PVP/Pt is very similar to the spectrum of pure PVP since steric considerations suggest that only a small number of the pyrrolidone rings are able to interact with the Pt surface (Figure 1A,B). It is worth noting that the only new feature in the FTIR-DRIFT spectrum of PVP/Pt is an additional band at 2043 cm^{-1} that may be attributed to edge-bound carbon monoxide formed during the polyol synthesis of Pt nanocrystals stabilized by PVP. Experiments performed in situ showed that the frequency of chemisorbed CO shifted gradually from 2043 to 1996 cm^{-1} when PVP/Pt was subjected to reducing conditions at 90 °C. It is well established that ν(CO) depends on the oxidation state of surface Pt.[22,23]

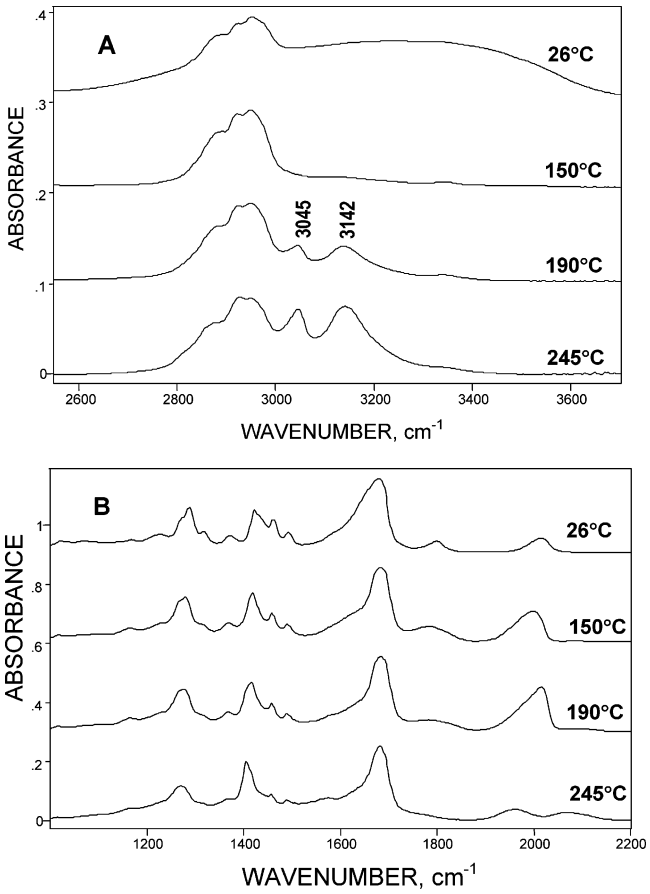

Figure 12. Thermodegradation of PVP/Pt (cubes, 7 nm) in H_2/Ar flow monitored by in situ FTIR spectroscopy. (A) Comparison of in situ FTIR spectra of PVP/Pt at selected temperatures between 26 and 245 °C in H_2/Ar flow; significant decomposition is observed at 245 °C. (B) Transformation of the FTIR spectrum of PVP/Pt in the region of CH_2 bending, amide stretch, and carbon monoxide vibrations in the temperature range of 26−245 °C.

Thermal Decomposition of PVP/Pt and PVP. The thermal stability of pure PVP has been extensively studied.[15,24,25] However, considerably less is known at the molecular level about the fate of capping PVP on the surface of Pt nanocrystals subjected to high-temperature treatment under reducing and oxidizing conditions that are standard procedure in heterogeneous catalyst preparation. Here we monitor in situ the transformation of PVP/Pt and pure PVP in the temperature range of 25−400 °C (heating rate 2 deg/min) in H_2/Ar (10% H_2) flow with FTIR-DRIFT technique. As can be seen in Figures 11 and 12, the spectra recorded upon thermal decomposition of PVP and PVP/Pt differ substantially. The sample of pure PVP was studied after removal of adsorbed water at 70 °C in a vacuum (10^{-5} Torr), and only after heating beyond 230 °C do significant changes in the C−H region become visible (Figure 11). While the position and intensity of the carbonyl stretch at 1680 cm^{-1} did not change, the intensity of the CH stretches relative to O═

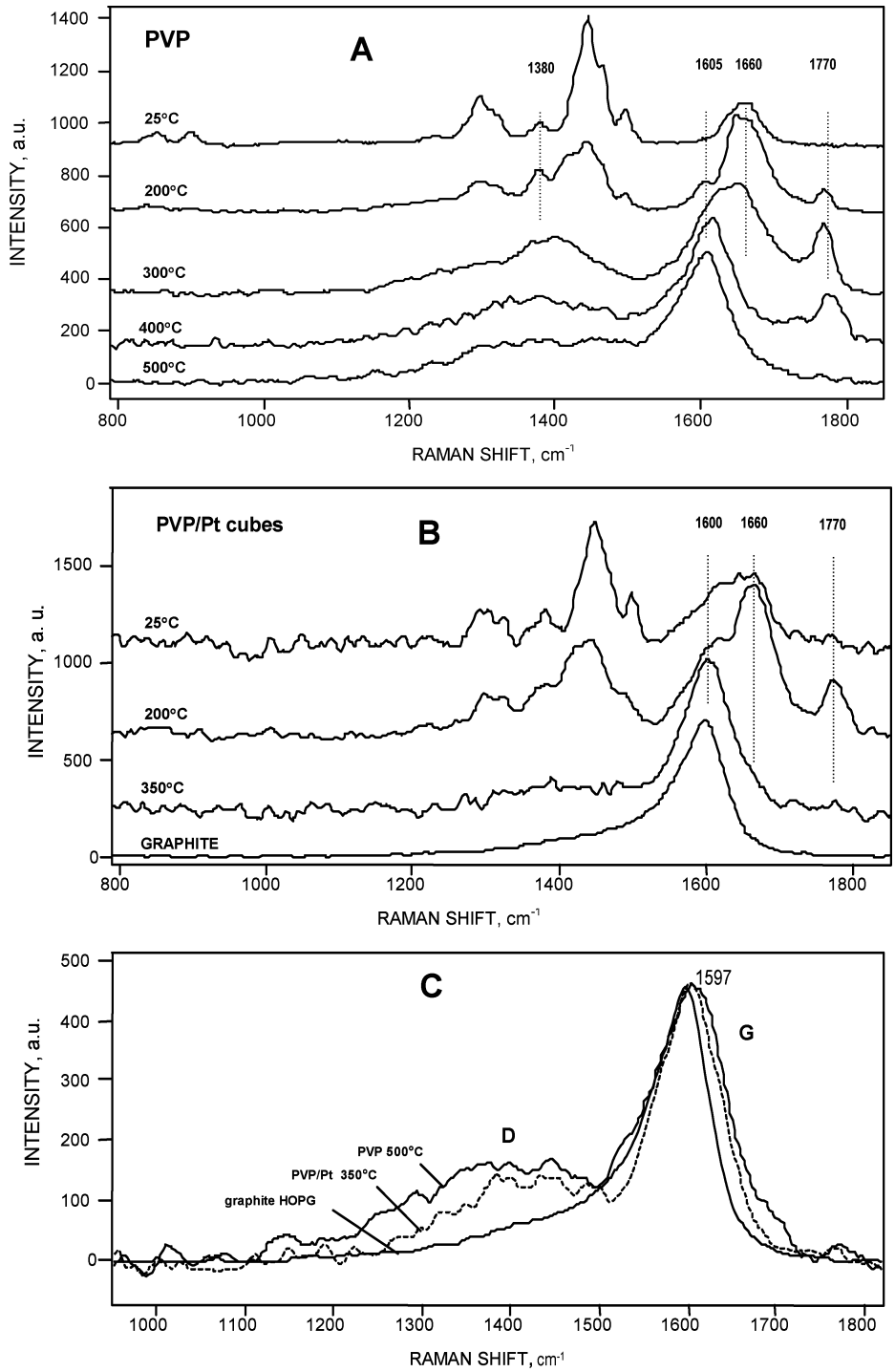

Figure 13. Thermodegradation of PVP and PVP/Pt in the air monitored by UV−Raman spectroscopy. (A) Overview spectra of PVP heated in the range of 25−500 °C. (B) Spectra of PVP/Pt heated in the range of 25−350 °C. (C) Comparison of UV−Raman (244 nm) spectra of HOPG graphite with final products of decomposition of PVP-500 °C and PVP/Pt-350 °C.

C< clearly decreased. It is believed that the pyrrolidone rings are stable at these temperatures, and that decomposition and cross-linking takes place mostly in the backbone chain. There is no evidence of ring opening.

By contrast, the changes in the spectrum of PVP/Pt are complex (Figure 12). We found that at 90 °C the band at 3400 cm^{-1} attributed to hydrogen-bonded water disappeared completely (Figure 12A). At 190 °C the band intensity of carbon monoxide (2012 cm^{-1}) reached a maximum and then decreased toward higher temperature (Figure 12B). Also above 170 °C, most CH stretch intensities of PVP decrease while two new bands appeared at 3142 and 3045 cm^{-1} that may be assigned to the N−H and C−H aromatic stretch absorptions, respectively (Figure 12A).[26] This suggests that the degradation of capping PVP occurs above 170 °C in H_2, and that it affects both the pyrrolidone rings and the backbone chain. We conclude that Pt nanocrystals catalyze the degradation of capping PVP in H_2/Ar flow. It is quite possible that hydrogen atoms formed during H_2 spillover on the platinum surface can initiate radical conversion of capping PVP. The presence of residual ethylene glycol or ascorbic acid oxidation products may also influence capping PVP degradation.

Oxidation of PVP and PVP/Pt in air was monitored with UV−Raman (Figure 13A,B). Two results should be noted. First,

at temperatures above 350 °C both PVP and PVP/Pt degrade to amorphous carbon. Furthermore, carbon forms on PVP/Pt at a lower temperature (300 °C) than in the case of pure PVP (450 °C). The amorphous carbon shows two peaks commonly labeled as G and D. The G peak is due to the bond stretching of pairs of sp^2 atoms and the D peak is due to the breathing modes of sp^2 atoms in rings.[27] The weaker D peak relative to the G peak indicates a more graphite-like structure with less disorder. As can be seen in Figure 13C, the presence of platinum nanoparticles favors the formation of a graphitic structure at lower temperatures.

Conclusions

We have shown that UV−Raman and FTIR spectroscopy are useful for monitoring the interaction of capping PVP with Pt nanocrystals. Specifically, deep UV−Raman (244 nm) is capable of detecting the vibrational modes related to amide group and ring vibrations, which may be assigned to "first-layer" pyrrolidone rings chemically bonded to the platinum surface. This selective enhancement is due to a combination of the resonance Raman effect and charge-transfer (or chemically) enhanced SERS effect, supported by (i) the energy of the 244 nm excitation laser line which lies within the strong absorption band of PVP/Pt, (ii) a decrease of the pyrrolidone ring ν(C═O) frequency on the order of 60 cm^{-1} in strong >C═O→Pt bonds, and (iii) an intensity enhancement of the first overtone of ν-(C═O) at 3200 cm^{-1} comparable to the intensity of fundamental mode, which is characteristic of the CT-SERS effect. The distinction between the CH_2 stretching modes for the pyrrolidone ring and backbone chain of PVP/Pt was made based on the selective appearance of ring peaks at 2964 and 2900 cm^{-1}.

Under reducing conditions platinum nanocrystals initiate the modification and decomposition of the capping agent, PVP, at about 100 °C below that of pure PVP. Starting at 150 °C for PVP/Pt, degradation of the backbone proceeds together with aromatic moiety formation. Under oxidative conditions, both PVP/Pt and PVP degrade to form amorphous carbon, although the decomposition of PVP/Pt proceeds at a lower temperature (300 °C) than for pure PVP (450 °C).

Acknowledgment. This work was supported by the Director, Office of Science, Office of Basic Energy Sciences, Division of Chemical Sciences, Geological and Biosciences of the U.S. Department of Energy under Contract No. DE-AC02-05CH11231

References and Notes

(1) Barton, J. K.; Rabinowitz, H. N.; Szalda, D. J.; Lippard, S. J. *J. Am. Chem. Soc.* **1977**, *99*, 2827. Matsumoto, K.; Fuwa, K. *J. Am. Chem. Soc.* **1982**, *104*, 897. Sakai, K.; Tanaka, Y.; Tsuchiya, Y.; Hirata, K.; Tsubomura, T.; Iijima, S.; Bhattachardjee, A. *J. Am. Chem. Soc.* **1998**, *120*, 8366.

(2) O'Halloran, T. V.; Roberts, M. M.; Lippard, S. J. *Inorg. Chem.* **1986**, *25*, 957.

(3) Matsumoto, K.; Takahashi, H.; Fuwa, K. *J. Am. Chem. Soc.*. **1984**, *106*, 2049.

(4) Hollis, L. S.; Lippard, S. *J. Am. Chem. Soc.* **1981**, *103*, 6761. Hollis, L. S.; Lippard, S. *J. Inorg. Chem.* **1993**, *22*, 2605.

(5) Rosenberg, B. *Cancer Chemother. Rep. Part 1* **1975**, *59*, 589. Rosenberg, B.; Van Camp, L.; Trosko, J. E.; Mansour, V. H. *Nature* **1969**, *222*, 385.

(6) Sakai, K.; Kizaki, Y.; Tanaka, Y.; Tsubomura, T.; Matsumoto, K. *J. Mol. Catal.* **1993**, *79*, 141.

(7) Fievet, F.; Lagier, J. P.; Blin, B.; Beaudoin, M.; Figlarz, M. *Solid State Ionics* **1989**, *32/33*, 198. Viau, G.; Fievet-Vincent, F.; Fievet, F. *Solid State Ionics* **1996**, *84*, 259.

(8) (a) Song, H.; Kim, F.; Connor, S.; Somorjai, G, A.; Yang, P. *J. Phys. Chem. B* **2005**, *109*, 188. (b) Wiley, B.; Sun, Y.; Mayers, B.; Xia, Y. *Chem.—Eur. J.* **2005**, *11*, 454. (c) Mayer, A. B. R. *Polym. Adv. Technol.* **2001**, *12*, 96. (d) Hirai, H.; Chawanya, H.; Toshima, N. *React. Polym.* **1985**, *3*, 127.

(9) (a) Bonet, F.; Tekaia-Elhsissen, K.; Sarathy, K. V. *Bull. Mater. Sci.* **2000**, *23/3*, 165. (b) Jiang, P.; Li, S.-Y.; Xie S.-S.; Gao, Y.; Song, L. *Chem.—Eur. J.* **2004**, *10*, 4817. (c) Henglein, A.; Erschov, B. G.; Malow, M. *J. Phys. Chem.* **1995**, *99*, 14129. (d) Narayanan, R.; El-Saed, M. A. *J. Phys. Chem. B* **2005**, *109*, 18460. (e) Lepp, A.; Siiman, O. *J. Phys. Chem.* **1985**, *89*, 3494.

(10) Lai, Y.-C. J. *Appl. Polym. Sci.* **1997**, *66*, 1475. Kminek, I.; Yagci, Y.; Schnabel, W. *Polym. Bull.* (*Berlin*) **1992**, *29*, 277.

(11) Taylor, L. S.; Langkilde, F. W.; Zografi, G. *J. Pharm. Sci.* **2001**, *90*, 888.

(12) BASF-PHARMA. *Technical Information*, MEMP 030753e, July 2, 2005.

(13) Tanaka, N.; Ito, K.; Kitano, H. *Macromol. Chem. Phys.* **1994**, *195*, 3369.

(14) De Faria, D. L. A.; Gil, H. A. C.; de Queiroz, A. A. A. *J. Mol. Struct.* **1999**, *479*, 9314.

(15) Yoshida, M.; Prasad, P. N. *Appl. Opt.* **1996**, *35/9*, 1500.

(16) Moskovits, M. *Rev. Mod. Phys.* **1985**, *57/3*, 783.

(17) Campion, A.; Kambhampati, P. *Chem. Soc. Rev.* **1998**, *27*, 241.

(18) Kneipp, K.; Kneipp, H.; Itzkan, I.; Dasari, R. R. *J. Phys.: Condens. Matter* **2002**, *14*, R597.

(19) Albrecht, A. C. *J. Chem. Phys.* **1961**, *34/5*, 1476.

(20) Clark, R. J. H.; Dines, T. J. *Angew. Chem., Int. Ed. Engl.* **1986**, *25*, 131.

(21) Arenas, J. F.; Woolley, M. S.; Tocon, I. L.; Otero, J. C. *J. Chem. Phys.* **2000**, *112/17*, 7669.

(22) Bauschlicher, C. W.; Bagus, P. S. *J. Chem. Phys.* **1984**, *81/12*, 5889.

(23) Zhou, M.; Andrews, L.; Bauschlicher, C. W. *Chem. Rev.* **2001**, *101/7*, 1931.

(24) Scheirs, J.; Bigger, S. W.; Then, E. T. H.; Billingham, N. C. *J. Polym. Sci., Part B: Polym. Phys.* **1993**, *31*, 287.

(25) Peniche, C.; Zaldivar, D.; Pazos, M.; Paz, S.; Bulay, A.; Roman, J. S *J. Appl. Polym. Sci.* **1993**, *50*, 485.

(26) Bellamy, L. J. *The Infrared Spectra of Complex Molecules*; Chapman and Hall: London, UK, 1975. Du, Y. K.; Yang, P.; Mou, Z. G.; Hua, N. P.; Jiang, L. *J. Appl. Polym. Sci.* **2006**, *99*, 23.

(27) Ferrari, A. C.; Robertson, *J. Phys. Rev. B* **2001**, *64/7*, 75414.

(28) Matthews, M. J.; Pimenta, M. A.; Dresselhaus, M. S.; Endo, M. *Phys. Rev. B* **1999**, *59/10*, R6585.

(29) McDermott, D. P. *J. Phys. Chem.* **1986**, *90*, 2569.